

# Characterization of Field-Emission Cathodes Based on Graphene Films on SiC

R. V. Konakova<sup>a</sup>, O. B. Okhrimenko<sup>a\*</sup>, A. M. Svetlichnyi<sup>b</sup>, O. A. Ageev<sup>b</sup>, E. Yu. Volkov<sup>b</sup>,  
 A. S. Kolomiitsev<sup>b</sup>, I. L. Jityaev<sup>b</sup>, and O. B. Spiridonov<sup>c</sup>

<sup>a</sup> Lashkaryov Institute of Semiconductor Physics, National Academy of Sciences, pr. Nauki 41, Kyiv, 03028 Ukraine

<sup>b</sup> Taganrog Institute of Technology, Southern Federal University, Taganrog, 347900 Russia

<sup>c</sup> Southern Laser Technology Center, Taganrog, 347900 Russia

\*e-mail: olga@isp.kiev.ua

Submitted February 4, 2015; accepted for publication February 19, 2015

**Abstract**—The properties of a point field-emission cathode representing a structure in the form of a silicon carbide tip coated with a thin graphene film are assessed. For the point cathode with the graphene coating, the current–voltage characteristics are constructed in the Fowler–Nordheim coordinates; the work functions  $\phi$  of the point cathode are calculated by their slope. The possibility of forming heavily doped  $n^+$ -SiC on the point surface by the sublimation of low-threshold field emission cathodes with low threshold electric fields and field-emission currents is shown.

DOI: 10.1134/S1063782615090146

## 1. INTRODUCTION

Over the last few years, field emission of cathodes made of carbon materials: fullerenes, nanodiamonds, nanotubes, glassy carbon, graphene-like materials, and graphene films, have been actively studied. This is due to the possibility of the development of a number of field-emission displays, micro- and nanosensors, and next-generation computers based on carbon field-emission cathodes [1]. Among all the above-listed materials, carbon nanotubes and graphene films are considered as most promising for the development of field-emission structures of micro- and nanoelectronics (point cathodes).

This is related to the high carrier mobility, conductivity, thermal conductivity, strength, and the radiation and thermal stability of graphene [2]. However, graphene films, despite great interest in their application as coatings for point cathodes, have not been adequately studied. This is mostly associated with difficulties in technological processes of the fabrication of graphene films themselves and nanoscale field-emission structures on their basis. A very important factor is also the choice of the substrate on which the graphene film is formed. As shown in [3, 4], the most successful combination of the possibilities of technology and obtained structural and optical properties of graphene is the formation of graphene films on a SiC surface by the sublimation method. In [5], this method was used to grow graphene films on conductive and semi-insulating substrates 6H-SiC; the annealing conditions allowed the fabrication of the least strained graphene layers on SiC.

The objective of this work is the development and study of prototypes of field-emission cathodes based on the graphene films on a heavily doped  $n^+$ -6H-SiC substrate grown by the sublimation epitaxy method [3–5].

## 2. METHODOLOGICAL ASPECTS OF SAMPLE FABRICATION AND MEASUREMENTS

Graphene films were grown by the technique described in [3–5]. As substrates, 6H-SiC samples doped with nitrogen to a concentration of  $\sim 5 \times 10^{18} \text{ cm}^{-3}$  were used. To remove silicon oxide from the SiC surface, the samples were annealed at a temperature of 900°C for 2 hours. Then the samples were annealed in vacuum at  $T = 1250^\circ\text{C}$  for 20 min.

The presence of graphene on the SiC surface, its degree of perfection, and the film thickness were estimated by Raman scattering (RS) spectra. The results of these studies were published previously in [5]. It was shown that annealing at a temperature of 1250°C promotes the formation of a graphene film with film-forming cluster sizes of  $\sim 10 \text{ nm}$ .

The graphene-film surface morphology was studied using a high-vacuum ( $\sim 10^{-7} \text{ Pa}$ ) scanning probe microscope (SPM) module (Nanofab NTK-9, NT-MDT). Figure 1 shows atomic-force microscopy (AFM) images of the 6H-SiC substrate surface after annealing at  $T = 900$  and  $1250^\circ\text{C}$ . We can see that a step structure typical of graphene films was formed on the SiC surface after annealing at  $T = 1250^\circ\text{C}$  [4, 6, 7].

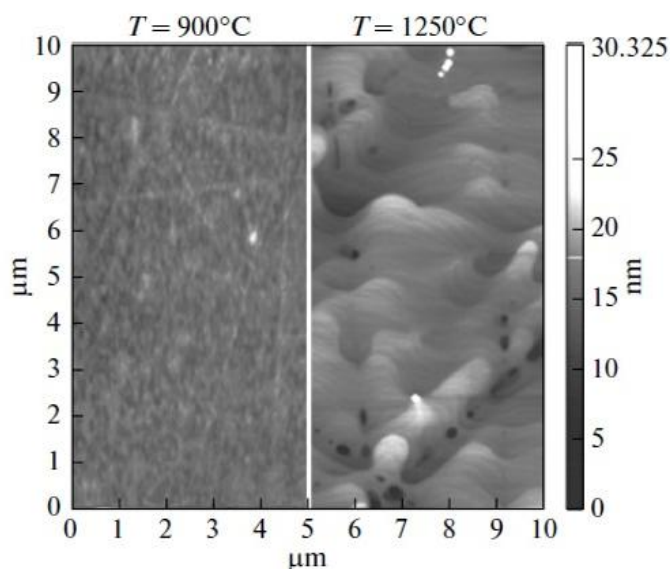


Fig. 1. AFM images of the 6H-SiC substrates after annealing.

Prototypes of point emission cathodes were fabricated by focused ion beams using a Nova Nanolab 600 system [8] at an accelerating voltage of 30 keV and an ion-beam current of 30 pA–3 nA. The cathodes were fabricated with tip radii of 20, 30, and 40 nm. To avoid possible graphene contamination during etching by gallium and silicon-carbide particles, graphene was grown on the emitter tip after fabrication of a cathode with the required sizes. Using a scanning electron microscope (SEM), which was a component of the system, images of the fabricated emission structures were obtained. Figure 2 shows the general view of the fabricated field-emission cathode and an image of the field-emission cathode tip with a radius of 40 nm.

3. EXPERIMENTAL RESULTS

The current–voltage (*I–V*) characteristics of the tip structures were measured using an Ntegra Vita scanning probe nanolaboratory at fixed interelectrode distances of 1, 3, and 5 nm. Figure 3 shows the *I–V* characteristic of the field emission cathode–probe system with a cathode-tip radius of *r* = 40 nm at interelectrode distances of 1, 3, and 5 nm.

We can see in Fig. 3 that electron emission is observed at low voltages. The field gain at interelectrode distances of 1, 3, and 5 nm was  $1.01 \times 10^9$ ,  $3.43 \times 10^8$ , and  $2.09 \times 10^8$  V/m, respectively. The emitting surface areas and field-emission current densities were calculated. It was found that the emitting surface area, depending on the applied voltage, can reach  $6 \times 10^{-15}$  m<sup>2</sup> at *U* = 10 V; in this case, the dependence *S* = *f*(*U*) is almost linear (Fig. 4a). As the voltage increases, the field-emission current density increases to  $\sim 4 \times 10^6$  A/m<sup>2</sup> at an interelectrode distance of 1 nm. Figure 4b (curves 1 and 2) shows the limitation of an increase in

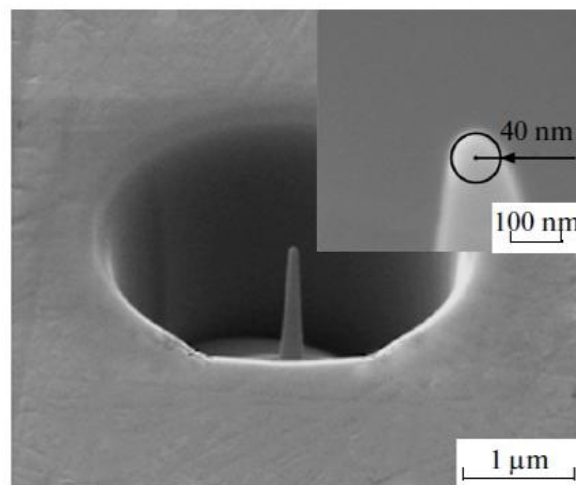


Fig. 2. SEM image of the obtained field-emission cathode.

the emission current density at voltages above 8 V. This is caused by features of the experimental setup. The maximum current is limited by 20 nA.

To analyze the characteristics of the field-emission prototype, the *I–V* characteristics were constructed in the Fowler–Nordheim coordinates:

$$\ln\left(\frac{J}{E^2}\right) = f\left(\frac{1}{E}\right),$$

where *J* is the current density and *E* is the electric field strength. The *I–V* characteristics constructed in the Fowler–Nordheim coordinates have a linear appearance (Fig. 5), which is typical of field emission. The work functions  $\phi$  of the point cathode were calculated by the slope of the *I–V* characteristics shown in Fig. 5.

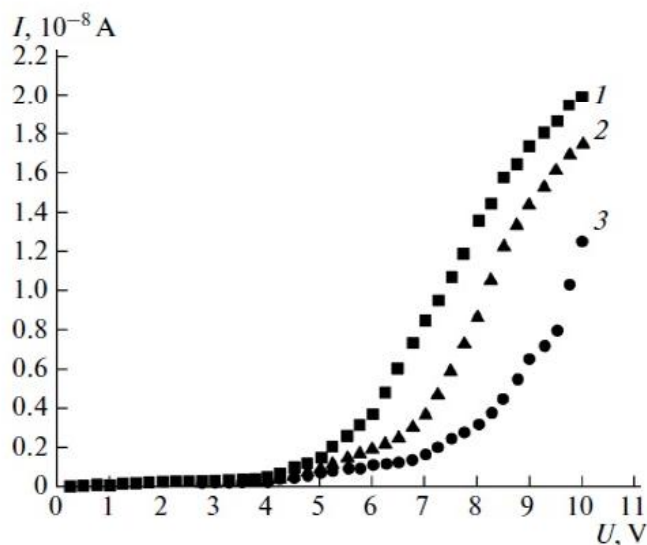


Fig. 3. Current–voltage characteristics of the field-emission cathode–probe system at interelectrode distances of (1) 1 nm, (2) 3 nm, and (3) 5 nm.

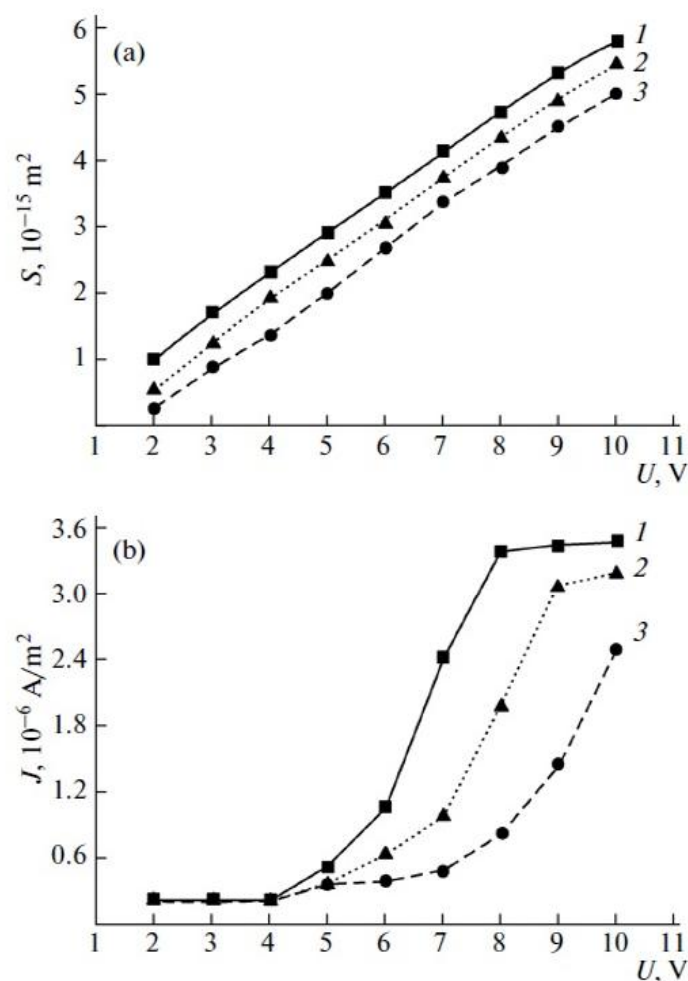


Fig. 4. Dependence of the (a) emitting surface area and (b) field-emission current density on the voltage in the emission-cathode–probe system at interelectrode distances of (1) 1 nm, (2) 3 nm, and (3) 5 nm.

The work functions of the field-emission cathode with a tip radius of 40 nm are listed in the table.

Work-function estimations for cathode tip radii of 20 and 30 nm at interelectrode distances of 1, 3, and 5 nm showed values of the same order. We note that the work function of graphene, depending on the number of monolayers is 4.3–4.6 eV according to [9]. The minimum and maximum values of  $\phi$  are given in [9] for one monolayer and ten monolayers, respectively, which is identical to the corresponding value of crystalline graphite [9] and is close to  $\phi$  of silicon carbide. We observed values of  $\phi$  closer to those of graphene-like structures based on carbon nanotubes [11] or car-

Electron work function  $\phi$  of the point cathode with a curvature radius of 40 nm at various interelectrode distances

Parameter	Value		
Interelectrode distance, nm	1	3	5
Work function, eV	0.31	0.6	0.9

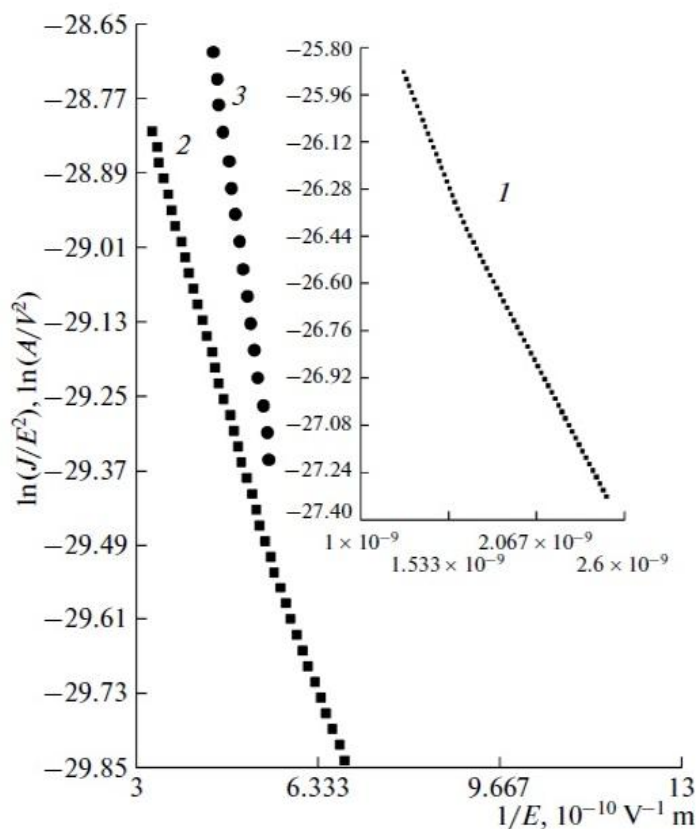


Fig. 5. Experimental current–voltage characteristic (Fig. 3) on the Fowler–Nordheim coordinates at interelectrode distances of (1) 1 nm, (2) 3 nm, and (3) 5 nm.

bon nanoclusters [10, 11]. In [1] and [11],  $\phi$  is 1 and 0.05–0.3 eV, respectively.

Indeed, provided that nanoclusters are field-emission sources as is considered in [10, 11], the graphene nanocluster sizes determined based on the RS data in our previous study [5] as  $\sim 10$  nm suggest that the rather low field emission observed in this study is caused specifically by graphene nanoclusters on the point cathode.

#### 4. CONCLUSIONS

It was shown that low-threshold field-emission cathodes can be formed based on graphene films grown on the tip surface of heavily doped  $n^+$ -SiC by the sublimation method. The observed threshold values of the electric field and field-emission current appeared significantly lower than those for ordinary point cathodes. Low-threshold field emission can be explained under the assumption of the presence of graphene nanoclusters on the point cathode surface. This assumption is confirmed by the comparatively low electron work function of graphene-coated point cathodes. The dependences of the emitting surface area and field-emission current density on the cathode–anode voltage were obtained. It was found that an increase in the voltage results in an increase in both the

area from which emission occurs and the current density. A decrease in the interelectrode distance led to a decrease in the work function, which made it possible to achieve higher emission currents, higher field-emission current densities, and larger emitting surface areas. The results of this study should be considered when developing devices of field emission micro- and nanoelectronics.

#### ACKNOWLEDGMENTS

The results of the study were obtained using equipment of the Shared Service Center and the “Nanotechnology” Science and Education Center of the Southern Federal University. The study was performed within the design part of the state task in the sphere of scientific activity (contract no. 16.1154.2014/K) and equipment of the Lashkaryov Institute of Semiconductor Physics of the National Academy of Sciences, Ukraine (contract on scientific and technical collaboration between the Lashkaryov Institute of Semiconductor Physics and the “Nanotechnology” Science and Education Center of the Southern Federal University for 2012–2014).

#### REFERENCES

1. Yu. V. Gulyaev, *Herald Russ. Acad. Sci.* **74**, 38 (2004).
2. M. Acik and Y. J. Chabal, *Jpn. J. Appl. Phys.* **50**, 070101 (2011).
3. A. A. Lebedev, I. S. Kotousova, A. V. Lavrent'ev, S. P. Lebedev, I. V. Makarenko, V. N. Petrov, and A. N. Titkov, *Phys. Solid State* **51**, 829 (2009).
4. A. A. Lebedev, I. S. Kotousova, and A. V. Lavrent'ev, *Phys. Solid State* **52**, 855 (2010).
5. R. V. Konakova, A. F. Kolomys, O. B. Okhrimenko, V. V. Strel'chuk, E. Yu. Volkov, M. N. Grigoriev, A. M. Svetlichnyi, and O. B. Spiridonov, *Semiconductors* **47**, 812 (2013).
6. G. M. Rutter, N. P. Guisinger, and J. N. Crain, *Phys. Rev. B* **76**, 235416 (2007).
7. J. Kedzierski, P. Hsu, and P. Healey, *IEEE Trans. Electron Dev.* **55**, 2078 (2008).
8. O. A. Ageev, A. S. Kolomiytsev, and B. G. Konoplev, *Semiconductors* **45**, 1709 (2011).
9. H. Hibino, H. Kageshima, and M. Nagase, *J. Phys. D: Appl. Phys.* **43**, 374005 (2010).
10. G. N. Fursei, V. I. Petrick, and D. V. Novikov, *Tech. Phys.* **54**, 1048 (2009).
11. G. N. Fursei, M. A. Polyakov, A. A. Kantonistov, A. M. Yafyasov, B. S. Pavlov, and V. B. Bozhevol'nov, *Tech. Phys.* **58**, 845 (2013).

*Translated by A. Kazantsev*